Supplementary materials

Fig. S1. Consort flow diagram of patient collective. The consort flow diagram illustrates how patients with colorectal liver metastases (CLM), who received neoadjuvant treatment, following liver resection between 2005 and 2011 in a curative intent at the Department of Surgery of the Medical University of Vienna, were retrospectively enrolled in this study.

Fig. S2. Representative example of computed areas of whole-slide tissue sections. Whole-slide tissue section of a CLM stained by IHC for CD45RO (brown color). Nuclei were counterstained (blue color). Two different regions were analyzed within the CLM: (i) tumor (TU) and (ii) invasive margin (IM; tumor/adjacent liver border). The clear distinguishable tumor area was marked manually. On the basis of the tumor area, a standardized invasive margin area with an exact width of 500 µm on each side of the tumor/adjacent liver border was created automatically by the analysis software. Scale bars 1 mm and 200 µm, respectively.

Fig. S3. Representative example for absolute cell quantification of whole-slide tissue sections. High resolution image (20x magnification) of a CLM stained by IHC for CD45RO (brown color). Nuclei were counterstained (blue color). (i) nuclei mask was programmed, which detects all single cells on the basis of the cell nuclei staining and morphology. This nuclei mask was further used for the generation of an (ii) antibody detection mask, identifying the antibody specific staining pattern (membrane, cytoplasmic or nucleus) of the differently used antibodies. Scale bar 20 µm.

Fig. S4. Representative example of pre- and postoperative therapy response evaluation. (A) Preoperative therapy response was evaluated by radiographic response, according to the response criteria in solid tumors (RECIST) 1.1 and morphologic response. (B) Contrast-enhanced computed tomography (CT) scan of a CLM (indicated by the black arrow) bevor neoadjuvant treatment (baseline). (C) Contrast-enhanced CT scan of a CLM

(indicated by the black arrow) after neoadjuvant treatment. According to the RECIST 1.1 criteria the patient was scored as stable disease (SD), whereas by the morphologic criteria as partial response (PR). (D) Postoperative therapy response was evaluated by pathologic response (Vitality), histologic response (TRG) and modified histologic response (mTRG). (E) Representative H&E staining of a CLM illustrating infarct-like necrosis (ILN; black diamonds), which characterizes a therapeutic response to chemotherapy compared to (F) usual necrosis (UN; black asterisks), indicating an insufficient treatment effect, which was considered as part of vital tumor cells. Scale bars 500 µm.

Fig. S5. DNA damage predicts radiomorphologic therapy response. (A) Comparison of marker panel between good and poor radiomorphologic responder is indicated by box-and-whisker plots and individual values (Mann-Whitney U test). Bolt horizontal line represents the median, top and bottom of the box illustrates the first and third quartiles, whisker represent 1.5 times the interquartile range (IQR). (B) Multivariate logistic regression model (LASSO) for the prediction of radiomorphologic response is illustrated by a receiver operating characteristic (ROC) curve. False positive rate (FPR) is specified at the abscissa and true positive rate (TPR) at the left ordinate. The ROC curve is color-coded according to the threshold values defined on the right ordinate. Black 45° line represents line of identity. Area under the curve (AUC) and corresponding p-values are indicated. (C) Comparison of the multivariate logistic regression model between good and poor radiomorphologic responder. CALR: calreticulin; DDX41: DEAD-box helicase 41; RIG-I: retinoic acid inducible gene I; GBP1: guanylate binding protein 1; cGAS: cyclic guanosine monophosphate adenosine monophosphate (GMP-AMP) synthase; Mx1: interferon-induced GTP-binding protein Mx1; p-eIF2α: phosphorylated-eukaryotic initiation factor 2 alpha; p-PKR: phosphorylated-protein kinase R; STING: stimulator of interferon genes; γH2AX: phosphorylated-histone H2AX

Fig. S6. ER stress, DNA sensor cGAS, functional type I and type II IFN system and activated DCs predict modified histologic therapy response. Comparison of marker

panel between good and poor (A) histologic and (D) modified histologic responder is indicated by box-and-whisker plots and individual values (Mann-Whitney U test). Bolt horizontal line represents the median (second quartile), top and bottom of the box illustrates the first and third quartiles, whisker represent 1.5 times the interquartile range (IQR). Multivariate logistic regression model (LASSO) for the prediction of (B) histologic and (E) modified histologic response is illustrated by a receiver operating characteristic (ROC) curve. False positive rate (FPR) is specified at the abscissa and true positive rate (TPR) at the left ordinate. The ROC curve is color-coded according to the threshold values defined on the right ordinate. Black 45° line represents line of identity. Area under the curve (AUC) and corresponding p-values are indicated. Comparison of the multivariate logistic regression model between good and poor (C) histologic and (F) modified histologic responder. CALR: calreticulin; DDX41: DEAD-box helicase 41; RIG-I: retinoic acid inducible gene I; GBP1: guanylate binding protein 1; cGAS: cyclic guanosine monophosphate adenosine monophosphate (GMP-AMP) synthase; Mx1: interferon-induced GTP-binding protein Mx1; p-eIF2α: phosphorylated-eukaryotic initiation factor 2 alpha; p-PKR: phosphorylated-protein kinase R; STING: stimulator of interferon genes; γH2AX: phosphorylated-histone H2AX

Table S1. Primer sequences used for mutation analysis.

KRAS: kirsten rat sarcoma viral oncogene homolog; BRAF: V-raf murine sarcoma viral oncogene homolog B1

Gen	Forward sequence	Reverse sequence
KRAS codon 12/13 (exon 2)	ACTGAATATAAACTTGTGGTAGTTGGACCT	TCAAAGAATGGTCCTGGACC
KRAS codon 61 (exon 3)	CTCAGGATTCCTACAGGAAGCAAG	TATCTTCAAATGATTTAGTATTATTTATGG
BRAF (exon 15)	CATAATGCTTGCTCTGATAGGA	CTAGTAACTCAGCAGCATCTC

Table S2. List of antibodies used for immunohistochemistry.

CALR: calreticulin; DDX41: DEAD-box helicase 41; DDX58: DEXD/H-box helicase 58; RIG-I: retinoic acid inducible gene I; GBP1: guanylate binding protein 1; MB21D1: Mab-21 domain

containing 1; cGAS: cyclic guanosine monophosphate-adenosine monophosphate (GMP-AMP) synthase; MLH1: mutL homolog 1; MSH2: mutS protein homolog 2; Mx1: interferon-induced GTP-binding protein Mx1; EIF2S1: eukaryotic translation initiation factor 2 subunit 1; p-eIF2α: phosphorylated-eukaryotic initiation factor 2 alpha; p-PKR: phosphorylated-protein kinase R; TMEM173: transmembrane Protein 173; STING: stimulator of interferon genes; γH2AX: phosphorylated-histone H2AX

Antibody	**Host**	**Clone**	**HIER buffer**	**Dilution**	**Company**
CALR	Mouse	FMC 75	Citrate pH 6	1:1359	Abcam
CD208	Rat	1010E1.01	Citrate pH 6	1:100	Dendritics
CD3	Rabbit	2GV6	ready to use pH 9	ready to use	Ventana
CD45RO	Mouse	UCHL-1	ready to use pH 9	1:200	BioGenex
CD8	Mouse	C8/144B	ready to use pH 9	1:75	Cell Marque
DDX41	Rabbit	EPR14298	Tris-EDTA pH 9	1:100	Abcam
DDX58 (RIG-I)	Rabbit	Polyclonal	Tris-EDTA pH 9	1:50	Abcam
GBP1	Mouse	1B2	ready to use pH 9	1:150	Abcam
Ki-67	Mouse	MIB-1	ready to use pH 9	1:200	Dako
MB21D1 (cGAS)	Rabbit	Polyclonal	Citrate pH 6	1:700	Sigma-Aldrich
MLH1	Mouse	M1	ready to use pH 8	ready to use	Ventana
MSH2	Mouse	G219-1129	ready to use pH 8	ready to use	Cell Marque
Mx1	Rabbit	Polyclonal	ready to use pH 9	1:150	Abcam
p-EIF2S1 (p-eIF2α)	Rabbit	E90	Citrate pH 6	1:50	Abcam
p-PKR	Mouse	E120	Tris-EDTA pH 9	1:500	Abcam
TMEM173 (STING)	Mouse	4E12	Citrate pH 6	1:200	Abcam
γH2AX	Mouse	9F3	Citrate pH 6	1:1000	Abcam
Anti-rat IgG	Rabbit	Polyclonal	not applicable	1:1000	Novus Biologicals

Table S3. Patient characteristics without imputed values estimated by the predictive mean matching method.

IQR: interquartile range; Left: descending colon, sigmoid colon or rectum; Right: caecum or ascending colon; Transverse: transverse colon; UICC: union for international cancer control; XELOX: capecitabine, oxaliplatin; XELIRI: capecitabine, irinotecan; FOLFOX: folinic acid, fluorouracil, oxaliplatin; FOLFIRI: folinic acid, fluorouracil, irinotecan; TOMOX: raltitrexed, oxaliplatin; CR: complete remission; PR: partial remission; SD: stable disease; PD: progressive disease; OR: optimal response; PR: partial response; AR: absent response; TRG: tumor regression grade; mTRG: modified tumor regression grade; KRAS: kirsten rat sarcoma viral oncogene homolog; BRAF: V-raf murine sarcoma viral oncogene homolog B1; CI: confidence interval

Demographics	**Total no (n=33)**
Median age ± IQR (years)	62 ± 19
Sex	
Male	17 (52%)
Female	16 (48%)
Primary tumor	
Tumor location	
Left	26 (12%)
Right	4 (79%)
Transverse	3 (9%)
pT stage	
pT1	2 (8%)
pT2	2 (8%)
pT3	20 (76%)
pT4	2 (8%)
pN stage	
pN0	11 (39%)

pN1	11 (39%)
pN2	6 (22%)
M stage	
M0	13 (42%)
M1	18 (58%)
UICC stage	
I	1 (4%)
II	4 (15%)
III	4 (15%)
IV	18 (66%)
Tumor differentiation	
Well	2 (8%)
Moderate	19 (70%)
Poor	6 (22%)
Residual Tumor classification	
R0	26 (100%)

Liver metastases	
Metastases timepoint	
Synchronous	19 (58%)
Metachronous	14 (42%)
Distribution	
Unilobular	15 (45%)
Bilobular	16 (49%)
Central	2 (6%)
Number of lesions	
Solitary	13 (39%)
Multiple	20 (61%)

Neoadjuvant chemotherapy	
XELOX	19 (58%)
FOLFIRI	4 (12%)
FOLFOX	4 (12%)
XELIRI	2 (6%)
TOMOX	1 (3%)
Fluorouracil	1 (3%)
Irinotecan	1 (3%)
Raltitrexed + Irinotecan	1 (3%)
Neoadjuvant bevacizumab	
Yes	29 (88%)
No	4 (12%)
Neoadjuvant cetuximab	
Yes	2 (6%)
No	31 (94%)
Median neoadjuvant cycles ± IQR	5 ± 3
Radiographic therapy response	
Good response (CR, PR)	15 (45%)
Poor response (SD, PD)	18 (55%)
Radiomorphologic therapy response	
Good response (OR, PR)	20 (60%)
Poor response (AR)	13 (40%)
Synchronous primary tumor resection	
Yes	2 (6%)
No	31 (94%)
Histology	
Adenocarcinoma - Tubular-papillary	27 (82%)
Adenocarcinoma - Mucinous	6 (12%)

Tumor differentiation		
Moderate	33	(100%)
Residual Tumor classification		
R0	33	(100%)
Pathologic therapy response		
Good response (0-25% viable)	9	(27%)
Poor response (≥25% viable)	24	(73%)
Histologic therapy response		
Good response (TRG 1-3)	4	(12%)
Poor response (TRG 4-5)	29	(88%)
Modified histologic therapy response		
Good response (mTRG 1-3)	17	(52%)
Poor response (mTRG 4-5)	16	(48%)
Mismatch repair status		
Proficient	33	(100%)
Deficient	0	(0%)
***KRAS* status**		
Wild-type	13	(39%)
Mutant	20	(61%)
***BRAF* status**		
Wild-type	33	(100%)
Mutant	0	(0%)
Median recurrence-free survival (months)	10	(95% CI 6.66-13.34)
Median overall survival (months)	40	(95% CI 26.50-53.51)

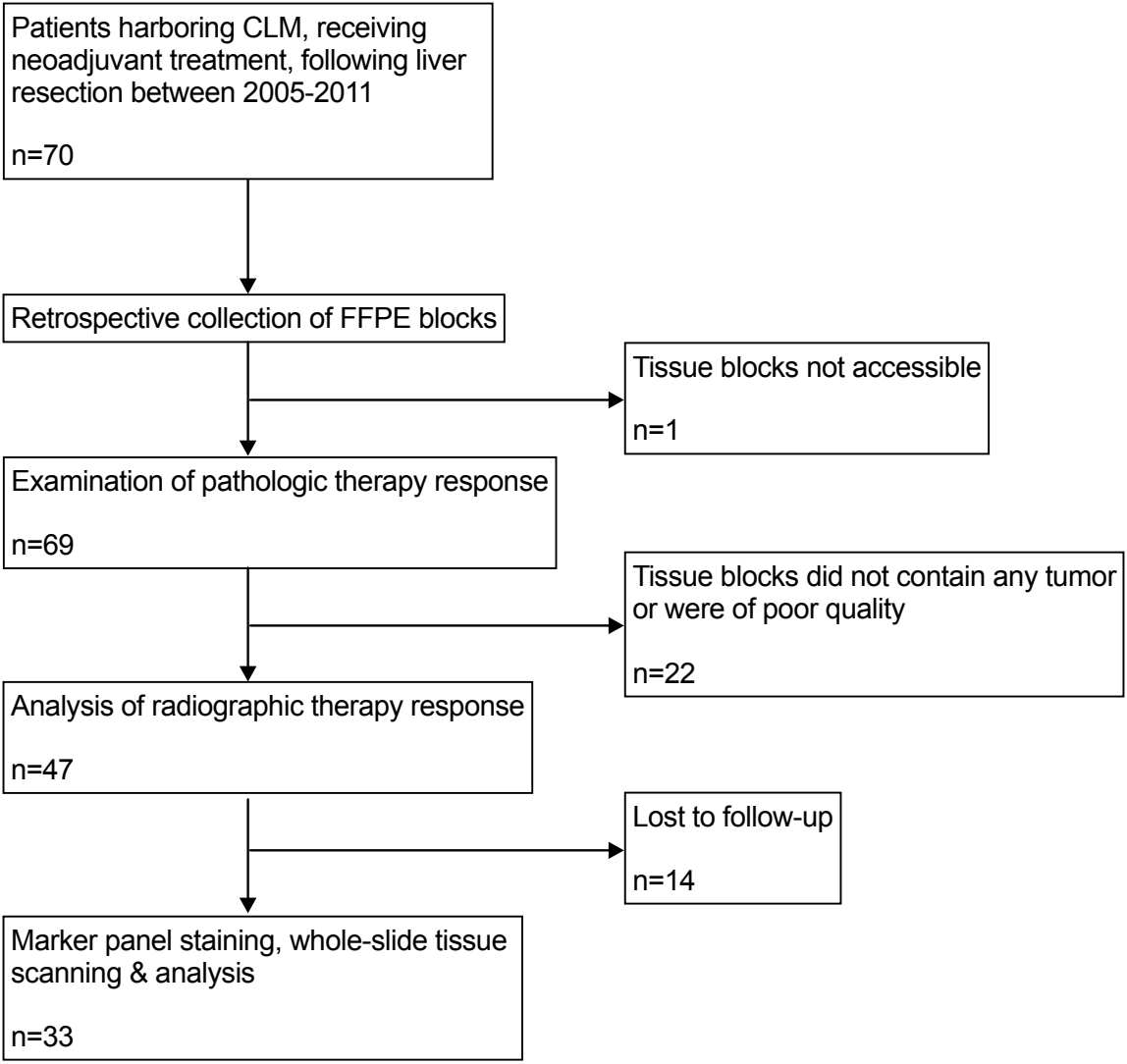
Patients harboring CLM, receiving neoadjuvant treatment, following liver resection between 2005-2011
n=70
Retrospective collection of FFPE blocks
Tissue blocks not accessible
n=1
Examination of pathologic therapy response
n=69
Tissue blocks did not contain any tumor or were of poor quality
n=22
Analysis of radiographic therapy response
n=47
Lost to follow-up
n=14
Marker panel staining, whole-slide tissue scanning & analysis
n=33

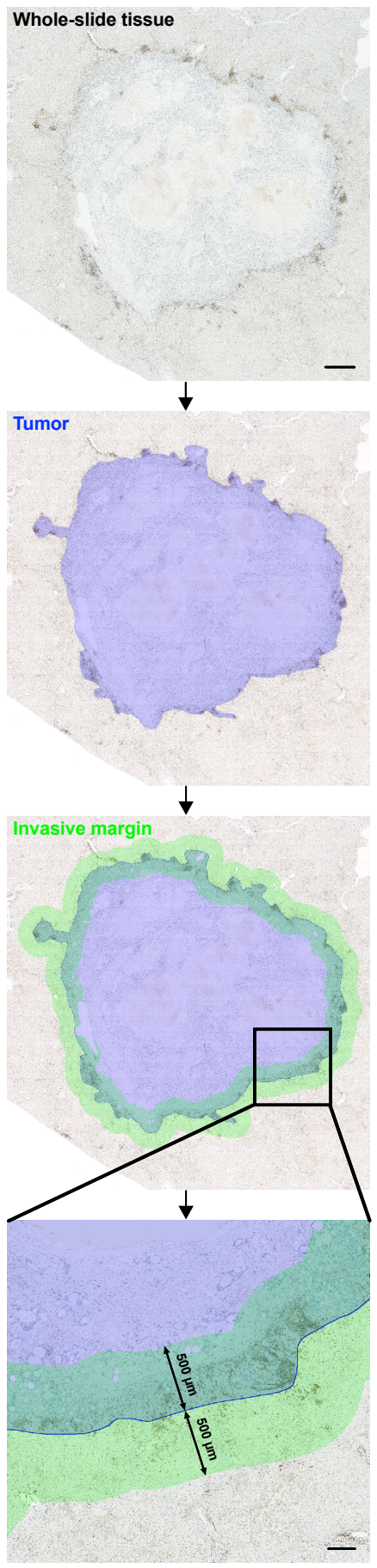
Whole-slide tissue
Tumor
Invasive margin
500 µm
500 µm

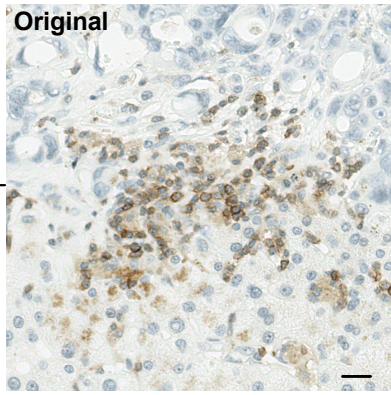
Original

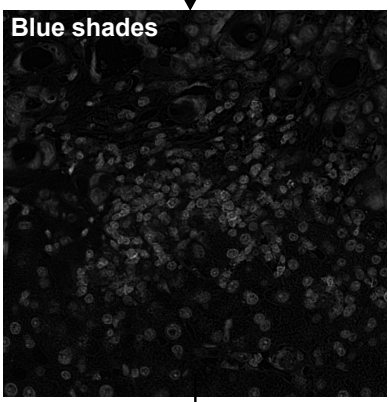
Blue shades

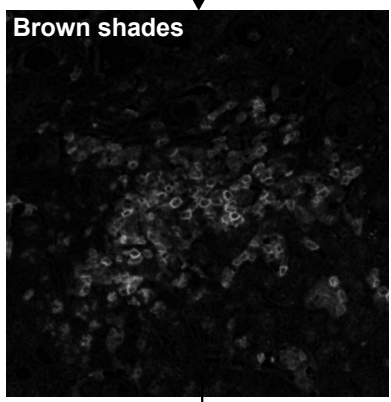
Brown shades

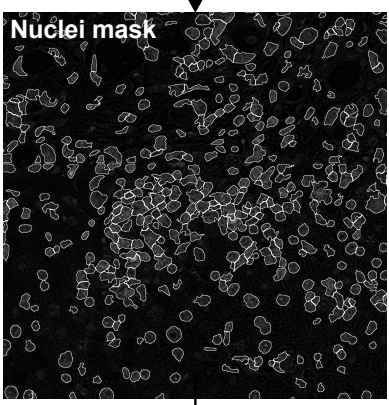
Nuclei mask

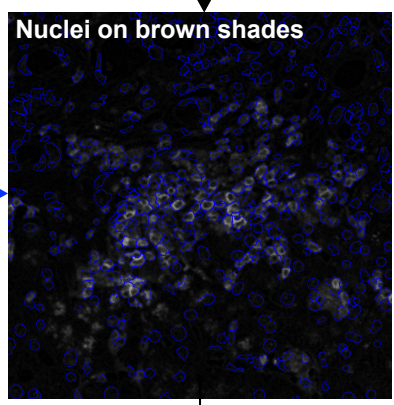
Nuclei on brown shades

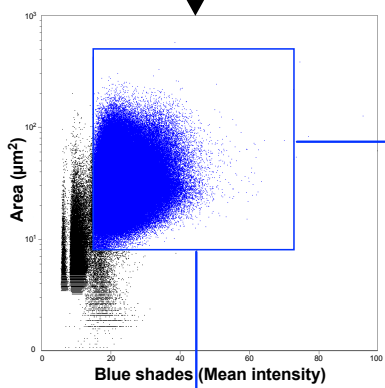
Area (µm²)
Blue shades (Mean intensity)

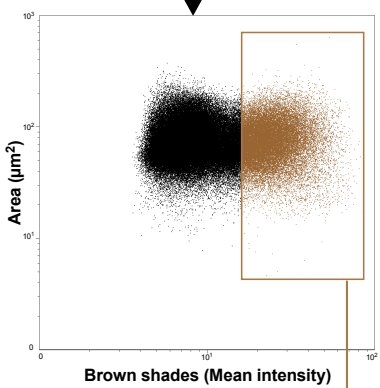
Area (µm²)
Brown shades (Mean intensity)

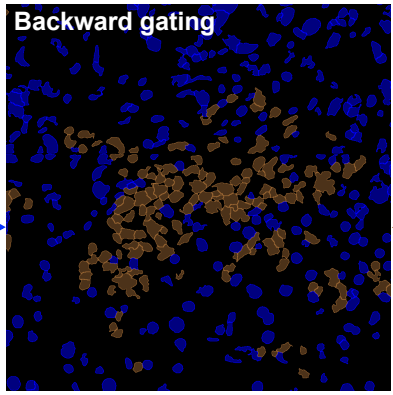
Backward gating

A

Preoperative therapy response evaluation

Radiographic response (RECIST 1.1)

Radiomorphologic response (Morphology)

D

Postoperative therapy response evaluation

Pathologic response (Vitality)

Histologic response (TRG)

Modified histologic response (mTRG)

B

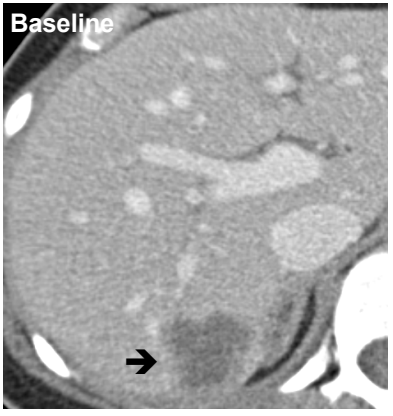

E

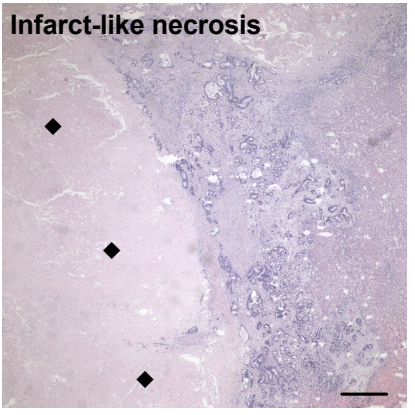

C

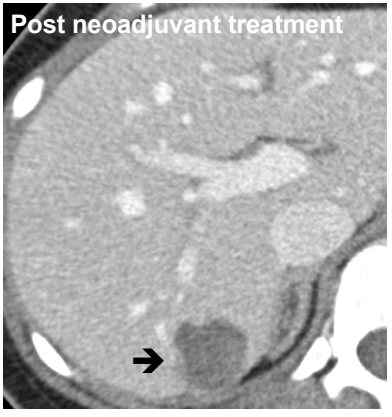

F

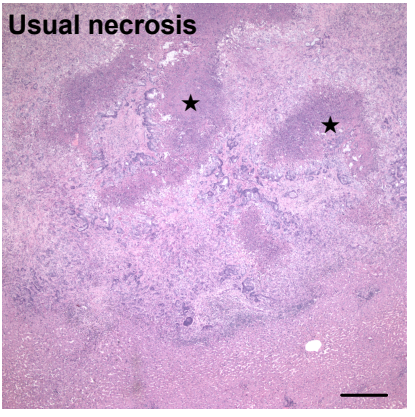

A

Preoperative therapy response evaluation

Radiomorphologic response (Morphology)

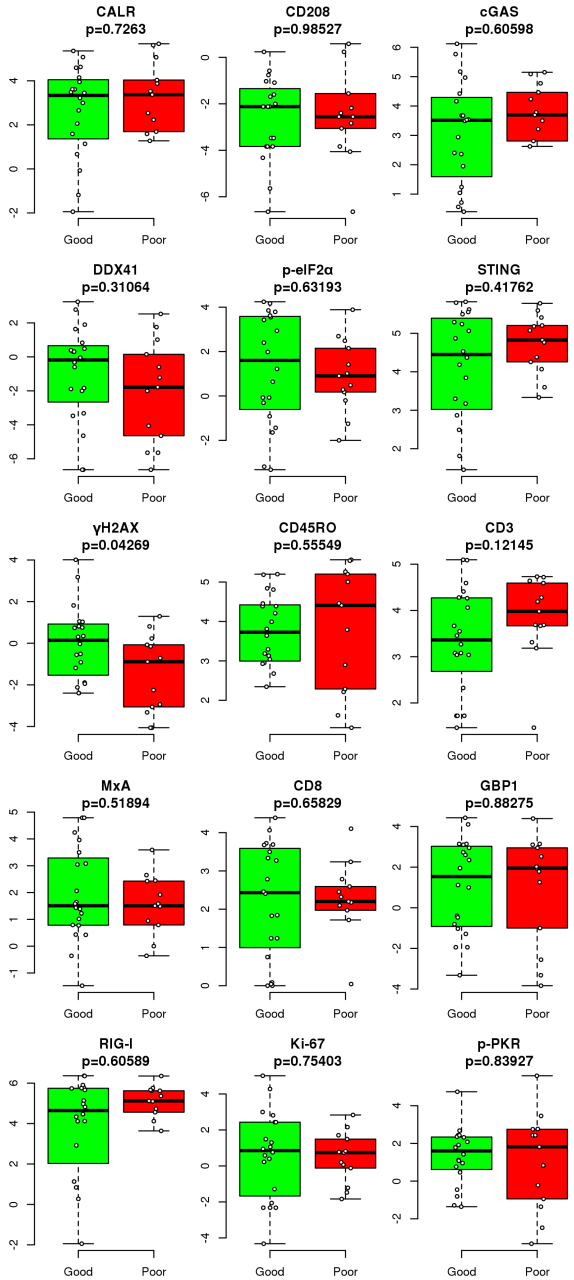

B

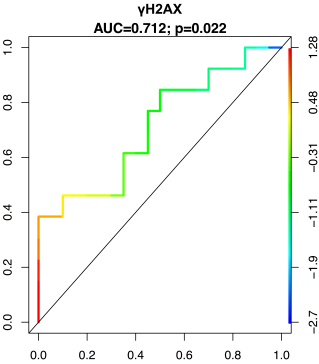

C

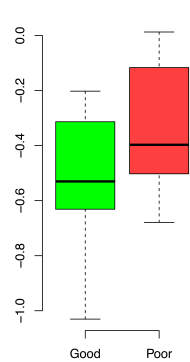

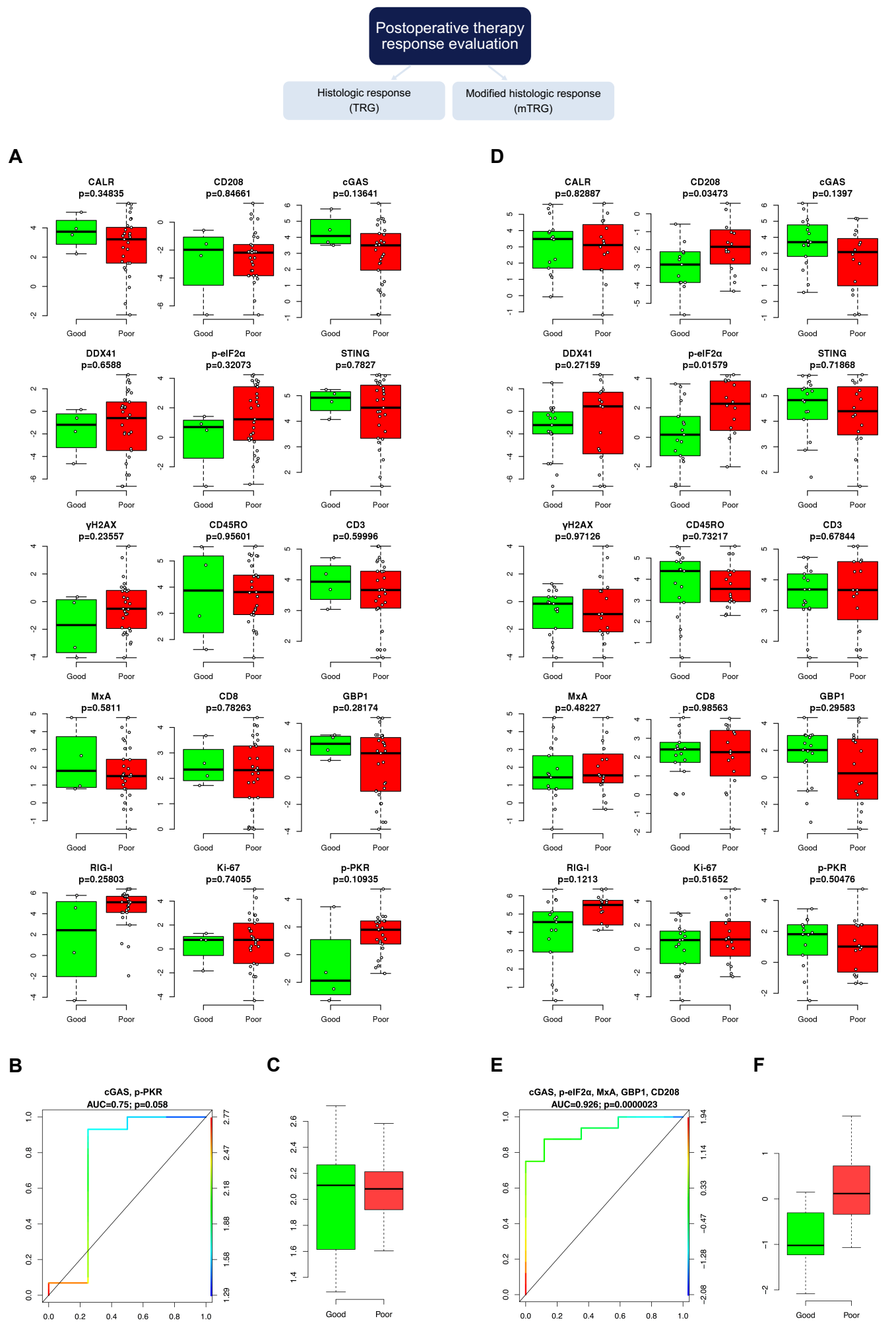
Postoperative therapy response evaluation
Histologic response (TRG)
Modified histologic response (mTRG)
A
CALR p=0.34835
CD208 p=0.84661
cGAS p=0.13641
DDX41 p=0.6588
p-eIF2α p=0.32073
STING p=0.7827
γH2AX p=0.23557
CD45RO p=0.95601
CD3 p=0.59996
MxA p=0.5811
CD8 p=0.78263
GBP1 p=0.28174
RIG-I p=0.25803
Ki-67 p=0.74055
p-PKR p=0.10935
D
CALR p=0.82887
CD208 p=0.03473
cGAS p=0.1397
DDX41 p=0.27159
p-eIF2α p=0.01579
STING p=0.71868
γH2AX p=0.97126
CD45RO p=0.73217
CD3 p=0.67844
MxA p=0.48227
CD8 p=0.98563
GBP1 p=0.29583
RIG-I p=0.1213
Ki-67 p=0.51652
p-PKR p=0.50476
Good
Poor
B
cGAS, p-PKR
AUC=0.75; p=0.058
C
E
cGAS, p-eIF2α, MxA, GBP1, CD208
AUC=0.926; p=0.0000023
F